Data informed physical models for district heating grids with distributed heat sources to understand thermal and hydraulic aspects

Natasa Nord [a], [*], Mohammad Shakerin [a], Tymofii Tereshchenko [b], Vittorio Verda [c], Romano Borchiellini [c]

[a] Department of Energy and Process Technology, Norwegian University of Science and Technology (NTNU), Kolbjørn Hejes Vei 1 B, Trondheim, 7491, Norway
[b] SWECO Norge AS, Trondheim, Norway
[c] Energy Center and Department of Energy, Politecnico di Torino, Turin, Italy

ARTICLE INFO

ABSTRACT

The aim of the study was to develop data informed physical models for simulation of district heating (DH) grids for better presentation of hydraulic and thermal aspects in the DH grids integrating heat prosumers. A DH grid organized as a ring and integrating a heat prosumer from a data center was analyzed. In this study, an extensive analysis for thermal and hydraulic aspects of theDH grid considering different configurations of distributed sources was performed. Different configurations for the prosumer connection, the return to return and the return to supply, together with the pressure and temperature control, were investigated. The results showed that increasing the share of renewable heat from the prosumer to the DH grid caused a pressure imbalance in substations close to it. Variable speed pump control was the solution for these issues and it gave up to 34% electricity savings. Lowering temperature levels in the DH network led to a decrease in DH heat losses of up to 14%. The return to supply configuration showed advantages in integrating the prosumer, as regards lower return temperatures and better waste heat utilization. The results indicated the main hydraulic and thermal features of integrating the prosumer in the DH grid.

1. Introduction

The use of renewable energy and waste energy is highly necessary to combat climate change [1]. Future district heating and cooling (DHC) systems may enable transition to a complete renewable society [2,3], meaning that they will be based on completely renewable energy, such as solar, waste heat and geothermal energy. In recent years, the role of district heating (DH) in future energy systems has been consistently studied, whether by statistical or analytical approaches, with a focus on parameters such as buildings' heat energy demand, possibilities of using local renewable energy sources (RES), design, control and management, etc. [2]. The conclusion is that DH has great potential to integrate RES, because DH can offer flexibility to the energy system, through synergies between waste-to-energy processes, and could ultimately provide secure, renewable, and in some cases more affordable, energy, compared to fossil fuels [4]. Flexibility can be

further enhanced through thermal storage units [5] and demand-side management [6]. In the review study of Werner, it is shown that DHC system are viable heat and cold supply options in a future world, while more efforts are required for identification, assessment, and implementation of these potentials in order to harvest the global benefits with district heating and cooling [7]. Compared to individual heat production by end users, DH systems are considered a more reliable, efficient and environmentally friendlier alternative solution to meeting space heating and domestic hot water demands [8]. For example, a comparison of heat production by DH systems and by individual heat production by using electric boilers in Norway shows that the DH solution results in lower CO_2 emissions [9]. Demand for heating in Norwegian buildings is expected to be up to 18% lower in all building types by 2050 [10]. This makes the efficient utilization of RES in DH even more essential, because DH will still be a promising solution for most users and should also meet the newest energy and environmental regulations.

Since future DH is depicted as sustainable energy systems using 100% RES, existing DH systems must be developed to meet the

* Corresponding author.
E-mail address: natasa.nord@ntnu.no (N. Nord).

Nomenclature		G	Mass flow rate kg/s
		M	Mass kg
Symbol	Definition Unit	R	Hydraulic resistance matrix bar
ρ	Density kg/m^3	P	Pressure vector bar
t	Pump input power vector W	Ω	perimeter m
p	Total pressure bar	U	Overall heat transfer coefficient W/m^2. K
r	Heat exchanger mass flow rate ratio	λ	Under-relaxation coefficient
T	Temperature K	ϕ	Heat load W
NTU	Number of heat transfer units	V	Volume m^3
c_p	Specific heat capacity kJ/kg.K	η_t	Heat exchanger efficiency
L	Length m	k	Heat exchanger hydraulic loss coefficient 1/m.kg
A	Incidence matrix	k_v	Valve hydraulic loss coefficient $[m.kg]^{1/2}$
K	Stiffness matrix		
f	Knowns vector		

upcoming requirements. A new actor has entered the DH market, called the "prosumer", that is a heat consumer able to act as a distributed heat source and cooperate in heat production by delivering heat to the main system [11]. Several heat prosumer types exist today and they can export small and large amounts of heat at different temperature levels [12]. The literature indicates some studies related to heat prosumers and their effects on the DH grid [10,13–16]. The most attractive for DH companies are big heat exporters with high temperature levels, like waste heat from industry, supermarkets or data centers. The growing number of data centers offers an incentive to utilize this excess heat in nearby facilities, and DH fits this aim perfectly [12]. Heat generation from data centers must be combined with the DH as a closed-loop system that will lead to heat recycling and minimum heat losses. Data centers act as huge electrical heaters, fed with electricity that further produces waste heat as a byproduct. A case study of integrating two retail stores and a data center as the distributed heat sources to a local grid of the DH system in Trondheim, Norway, was performed in Ref. [17]. In this study, the results show up to 25% of the annual heat demand being covered by prosumers and reduced annual heat loss, compared to scenarios without prosumers. The research in Ref. [18] addressed the integration of solar thermal collector prosumers in DH. The bidirectionality of prosumer-based DH systems was discussed via the application of decentralized pumps in a case study. The authors suggested that, to increase system efficiency of this network type, better operation and control of networks with prosumers is needed [18].

Regardless of all the above-mentioned advantages, there are two considerable technical problems with heat export from data centers: 1) relatively low export temperatures that do not fit with the current high temperature DH grids and 2) the difficulty in DH grid control. In order to increase the export temperature level, data centers utilize mechanical cooling with heat pumps. In that way, the evaporator side is used to provide cooling, while the condenser side is used to provide thermal energy of 55 °C–80 °C, which is suitable for further use. Depending on the application requirements, such as temperature level of a local DH grid combined with the heat export quantity, heat recycling from data centers may offer economic advantages. The prosumer in DH networks is a relatively new concept, and there are still several unsolved issues. Temperature oscillations in the network could take place and change in pressure level is inevitable. Increase in velocity within pipes is predictable when prosumers produce at their maximum, but pipe sizing is of great importance in smart DH grids [5]. A heat prosumer in the system causes pressure cones, which dramatically affect consumers, both near and far from a prosumer substation. In order to be able to harvest more heat from a prosumer, it is

suggested that a lower initial pressure gradient from the main plant be maintained; however, this consideration may cause low pressure on the customer side not affected by prosumers [15]. For this reason, there is a strong requirement for a detailed mathematical model, to investigate the effect of heat export on pressure and temperature levels in each node of a DH grid.

The operation of a DH grid may be analyzed once the physical characteristics involved in the DH distribution system are modeled in the proper way. In general, the theory behind various studies on DH grid operation is based on fluid mechanics theories to describe pressure drop, while heat transfer theory is used to explain thermal losses and temperature drops. Graph theory with a semi-implicit (SIMPLE) algorithm has been used in several studies to explain the behavior of DH grids [19–21]. Due to the requirement for high quality data, only a few operation points were analyzed in the literature, which does not give a true picture of the real operational data. To decrease the computational burden, a graph theory approach, combined with the proper orthogonal decomposition for the hydraulic part of the grid model, was implemented, to model a small DH system with one centralized source in Tannheim, Austria [22]. Despite the small average error of the model, the model was shown to be hardly able to follow the dynamic pattern of the DH network, because of the lack of pipe information and the model's calibration approach. A combination of a thermal dynamic model and a linear model for the pressure level was implemented in Ref. [23], to model a DH system with one centralized geothermal source, in Tianjin, China. The proposed approach seems to be capable of reflecting the real DH operation, but the number of customers has a strong impact on results. Linear models for the pressure level and heat losses with detailed input data for each time step may be efficient for modeling a DH grid [24]. However, for proper calibration, this approach requires good knowledge of the system, and any change in it will require model changes, to adapt to a new configuration. The impact of prosumers on the DH system in Malmo, Sweden, was studied by using NetSim in Refs. [14,15]. NetSim has a good user interface and was developed for engineers dealing with DH systems [25], but it can simulate a DH grid for specific scenarios and discover issues in a suggested scenario, without considering operational data over a longer time. Therefore, in this study, the most comprehensive methods for modeling of thermal systems [20], combined with heat load data for each time step, were employed to focus on DH grid operation and development.

Based on future trends in the DH sector, the transition to a renewable energy society depends on in-depth understanding of the effect of the heat prosumer on a DH system. Therefore, this study aimed to understand how the introduction of a heat

prosumer to the DH system affects the DH network performance, such as pressure and temperature distributions and thereby distribution losses. Due to the theoretically detailed approach related to practical problems and the huge amount of detailed measurement data, this work goes beyond the state of the art. The novelty and contribution of this study related to theoretical perspectives are data informed physical models for simulation of DH grids. With the data informed is meant that measurement data were strongly combined with the domain knowledge to develop reliable physical modes. Further, different configurations for the prosumer connection and control strategies were introduced to the model. The results may be further used for innovative solutions for the pressure and temperature control. Therefore, the novelty and contribution of this study related to engineering perspectives are discovery and presentation of hydraulic issues in the DH grids integrating heat prosumers. Finally, the study presents an extensive analysis for thermal and hydraulic aspects of the DH grid considering different configurations of distributed sources. The rest of the paper is structured as follows. First, the method is introduced. The case study and possible connection configurations to introduce the prosumer together with the grid control, are presented. Finally, the results and conclusions are presented.

2. Method

The analyzed DH grid at the university campus is organized as a ring and delivers heat to the university buildings via consumer substations in each building. A heat prosumer harvesting heat from a data center was integrated to the system. To utilized in the best way available measurement data, while providing physically relevant models, an approach for data informed physical models was suggested. To mathematically describe the analyzed DH grid, the DH grid and simplified constituent components were modeled. To model the performance of the DH grid, the continuity, the momentum, and the energy balance equations were used, as suggested in Ref. [20]. Further, one-dimensional model of the flow was assumed, together with graph theory [26,27], to present the connection between the objects. The simplified components included the following: a substation model, a valve model, circulation pump, a radiator model to estimate the return temperature of the heating system, and a heat prosumer model. The heat prosumer model was described as a heat pump model, based on the real performance data. Heat load data on an hourly basis were used as input. Monitoring data of temperatures and pressures were used to calibrate the model. The entire model was developed in MATLAB. The heat use data were provided from the energy monitoring platform of the campus, while the operation data on temperatures and pressures were provided from the campus' building energy monitoring system. Consequently, the proposed method has numerous advantages, such as: 1) easy to calibrate with the real measurements, 2) simple to understand and present relevant engineering issues such as pressure and temperature level, 3) simple

to identify relevant physical aspects of the DH grids.

To discuss the performance of the system and different configurations for including the prosumer, the temperature and pressure levels, together with mass flow rates, were the most important outputs of the model to be observed. The DH grid model consisted of two parts, the hydraulic model and the thermal model, as shown in Fig. 1. The grid topology was mathematically described by graph theory [26,27]. In this regard, the interconnection of nodes (junctions) and edges (pipe branches) was expressed by means of an "incidence matrix". The incidence matrix was constructed as a matrix with a number of rows, equal to the number of nodes in the grid, and columns at the size of the number of branches. Each element of the incidence matrix contained either +1 or −1, if the node was an inlet or outlet for the branch, and 0 if it was not connected to the branch. State properties, such as pressure and temperature, could be obtained at each node, while mass flow rates and velocities were defined at each node.

In the following text, models for each constituent element and the simulation set-up are explained.

2.1. Fluid dynamic model

The fluid dynamic model was developed as steady state. The reason for this approach was the availability of data on an hourly level, which led the system to rapidly reach the hydraulic balance. For a generic branch of the DH grid, hydraulic balance was derived as:

$$(p_{out} - p_{in}) = -\Delta p_{FRICT} - \Delta p_{LOCAL} + \Delta p_{PUMP} \tag{1}$$

where p_{in} and p_{out} are the total pressure levels in and out of the pipe. Δp_{FRICT} takes viscous force into account, Δp_{LOCAL} stands for the local pressure losses, and Δp_{PUMP} is the pressure increase over the circulation pump.

2.2. Thermal model

The following equations give general formulation of the one-dimensional time-variant energy conservation law, while neglecting the heat conduction along the length of the branch. In this study, heat losses at the pipe walls were assumed to be perpendicular to the assumed direction. Therefore, the heat exchange between the branch and the ground was considered a volumetric sink term ϕ_l, as the following:

$$\frac{\partial (\rho_j c_{p,i} T_i)}{\partial t} \Delta V_i + \sum_j G_j^t T_j^t c_{p,j} = -\phi_{l,i}^t \tag{2}$$

where T_i is the temperature of the ith node, while T_j is the temperature at the boundary of the control volume surrounding the ith node. t indicates the current time, forwarding with steps of Δt. Heat transfer through the walls to the surrounding, ϕ_l, is introduced as
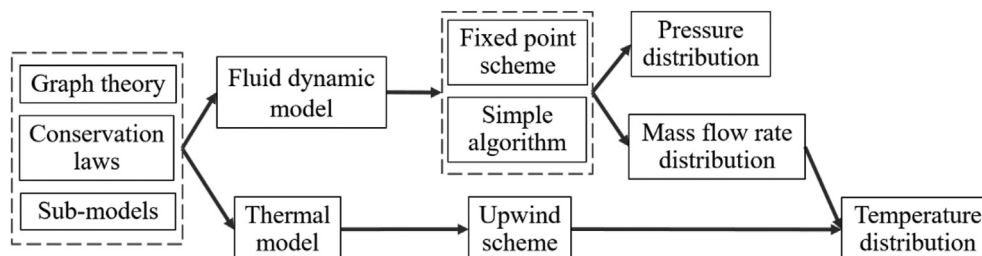

Fig. 1. Flowchart representing the workflow.

the following:

$$\phi_{l,i}^t = \sum_j \frac{L_j}{2} \Omega_j U_j (T_i^t - T_\infty^t) \tag{3}$$

where Ω_j is the perimeter of the branch, U_j is the overall heat transfer coefficient, and T_∞ is the temperature of the ground. In Equation (3), half of the branch length is considered.

2.3. Substation model

The consumer substations were modeled as one heat exchanger receiving total heat demand for an observed building. The aim was to find the return temperature at the primary side of the heat exchanger at each time interval. The return temperature at the primary side of the heat exchanger was necessary to define the mass flow rate for each building in the DH grid. The efficiency of a heat exchanger was defined in two ways, by using temperatures and by using properties of the heat exchanger such as:

$$\eta_t = \frac{T_{sp} - T_{rp}}{T_{sp} - T_{rs}} \tag{4}$$

$$\eta_t = \frac{1 - \exp((-NTU(1-r))}{1 - r\Gamma \exp((-NTU(1-r))} \tag{5}$$

where T_{sp}, T_{rp}, and T_{rs} are the supply temperature at the primary side, the return temperature at the primary side, and the return temperature at the secondary side of the heat exchanger, respectively. The return temperature at the secondary side of the heat exchanger was obtained by empirical relations. In Equation (5), r is the ratio of primary and secondary mass flow rates. NTU is the number of heat transfer units.

The rated performance data for the heat exchangers were provided for the following temperature levels: the supply and the return temperatures at the primary side of 90 °C and 65 °C, respectively, and the supply and the return temperatures at the secondary side of 60 °C and 40 °C, respectively. Based on Equations (4) and (5), the primary side return temperature, T_{rp}, was calculated.

A simplified model of the pressure drop at substations consisted of a heat exchanger pressure loss and a flow control valve, named Δp_{he} and Δp_v, respectively. These two pressure drops are given in Equations (6) and (7) as the following:

$$\Delta p_{he} = kG^2 \tag{6}$$

$$\sqrt{\Delta p_v} = \frac{G}{k_v} \tag{7}$$

In Equation (6), k is the pressure drop coefficient for the heat exchanger. In Equation (7), k_v determines the capacity of the valve and defines the volumetric flow rate through the valve. k_v was modeled by combining k_{vs} and the valve opening. k_{vs} was defined at the maximum flow rate, the full valve opening, and the corresponding pressure drop. In that way, the valve was modeled as the equal percentage and the relationship between the valve opening and the transferred heat rate of the consumer substation was linear, which is desired in engineering practice. Finally, the overall pressure drop, Δp_{USER}, at the substation was calculated as the sum of the pressure drop in the heat exchanger and the control valve.

2.4. Model for the waste heat from the data center

In this study, the model for the waste heat was developed by using one year of the monitoring data from a heat pump that was cooling the data center and providing waste heat to the DH grid at the same time. A compression refrigeration system was utilized in the data center, with ammonia as a working fluid. To utilize the condenser heat, a branch from the return line of the primary DH grid was coupled with the condenser.

The analyzed heat pump gave approximately 1 MW of the condenser heat for each 600 kW of cooling load. To define the model for the waste heat, the compressor power, the condenser heat, and the evaporator load were defined by interpolating the corresponding heat pump performance data to the return temperature of the DH grid. One year 15-min measurements were used to define the heat pump model. The defined models are presented in Fig. 2 as the functions of the return temperature. The interpolated functions from Fig. 2 were used further to calculate the condenser heat and other necessary performance data.

2.5. Simulation setup and boundary conditions

In this section, the equation systems, model calibration, and the simulation setup are explained.

The equation system for the mass conservation for each node in the matrix form is introduced as:

$$A \cdot G + G_{ext} = 0 \tag{8}$$

where A is the incidence matrix and G is the column vector that contains the mass flow rates of each branch. G_{ext} is the column vector, sized by the number of nodes. Considering a generic branch that connects nodes, the momentum equation in the matrix form is
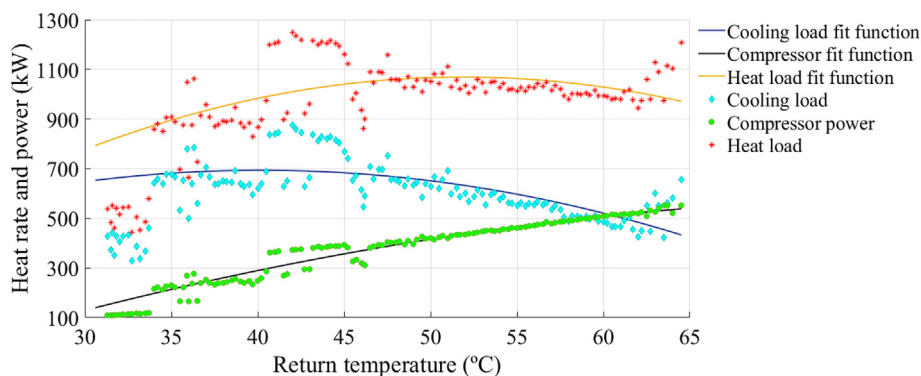

Fig. 2. Models for the condenser heat, evaporator load, and compressor power as the function of the return temperature in the DH grid.

obtained as:

$$A^T \cdot P = R \cdot G - t \tag{9}$$

where R is the diagonal matrix, considering hydraulic resistances due to local and viscous losses in each pipe branch. P is the column vector that contains the pressure of each node. The product of $A^T \cdot P$ defines the pressure difference between the inlet and outlet of each node. Matrix t contains the effect of pumps on each branch. Due to term R, the momentum Equation (9) is non-linear. In addition, the two equations (8) and (9) are coupled and need to be solved simultaneously. Therefore, the momentum Equation (9) cannot be solved explicitly. "SIMPLE-algorithm" (semi-implicit algorithm) [28], together with the fixed-point method [29], was adopted to find values for the pressures and the mass flow rates, P and G.

The thermal model is discretized. An upwind scheme was employed to solve the thermal problem. Since temperatures are defined at the nodes, the temperatures at the boundary are defined in accordance with the nodes, by means of the upwind scheme. According to the upwind scheme method, the temperature at each boundary is assumed equal to the temperature in the upstream node. The final set of N equations for the description of the thermal problem in the matrix form can be defined as:

$$\left(M^t + K^t\right) \cdot T^t = f^t + M^{t-\Delta t} \cdot T^{t-\Delta t} \tag{10}$$

where the diagonal matrix M is defined as $M(i,i) = \frac{\rho_i c_{p,i}}{\Delta t}$. K is called the stiffness matrix, and f is the vector of known terms in Equation (10). Since the flow rates in the DH grid are forced convectively by components such as pumps, continuity and momentum equations must be solved, to define P and G, prior to proceeding with the thermal analysis. The flowchart for the entire calculation procedure is given in Fig. 3.

To evaluate how different amount of heat exported to the DH grid would influence the DH pressure and temperature level, three test cases were developed by gradual increase of the flow rate through the prosumer. The aim of this was to evaluate how the DH grid would behave in the case of higher heat share from the pro-sumer. The cooling process in the data center made the waste heat almost always available at an approximately stable level during the year. The summary of the different test cases considering different flow rate through the prosumer is shown in Table 1.

In Table 1, $G_{C,des}$ is the mass flow rate of the water flowing through the heat pump condenser. G_{max} is the maximum mass flow rate of the DH grid and corresponded to the maximum heat demand.

In this study, the heat losses of the pipe were calibrated, based on the producer data for the design conditions, while, for the operation condition, the model results were combined with the measurement data. Further, the operation conditions were modeled by using the above models, while the input vectors of heat load for each time step were introduced from hour to hour. This approach was found to be sufficiently good to model a DH grid, because it utilized a detailed model of the DH grid and real mea-surements as shown in Ref. [24].

Regarding the boundary conditions, substations in the DH sys-tem were treated as boundary nodes. It was assumed that each building extracts/injects the mass flow rate from/to the DH grid via the substation. This meant that the control volume for the fluid dynamic and thermal model did not include the secondary side of the DH substation. The substations acted as known boundaries to the system of equations, if they were inlet to the supply or the return network.

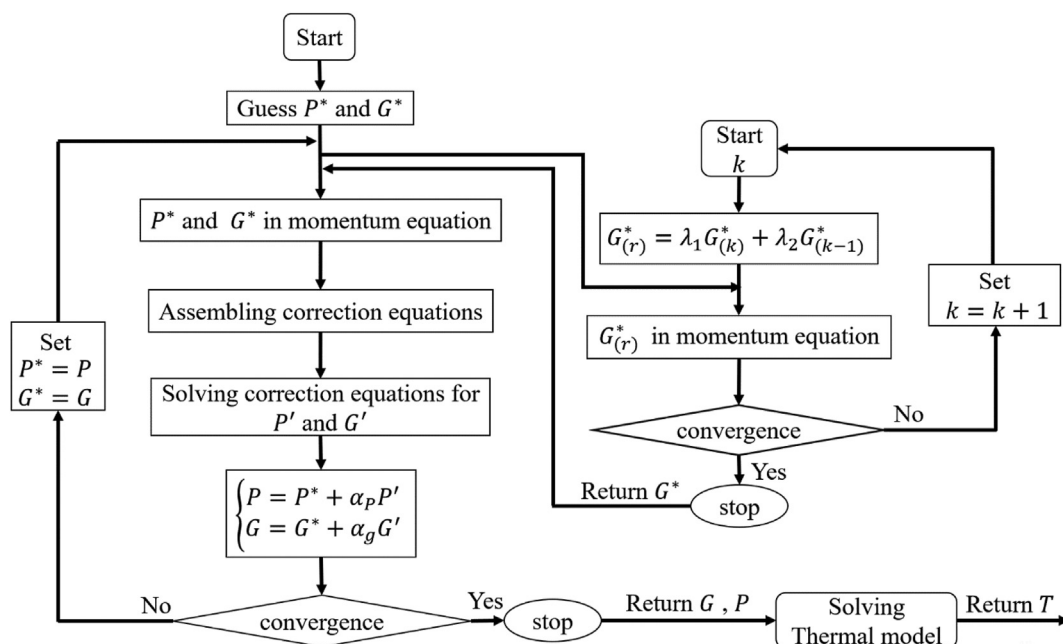For the analyzed DH grid, two types of connection

Table 1
Test cases for reflecting different shares of renewable energy source.

Case	$G_{C,des}$ (kg/s)	$G_{C,des}/G_{max}$ (%)	
		R2R	R2S
Case 1	10.2	9.5	10.5
Case 2	12.7	11.8	13.4
Case 3	15.5	14.4	16.9

Fig. 3. Flowchart of the SIMPLE algorithm (right) and fixed-point scheme (left).

configurations for the prosumer were analyzed, the return-to-return (R2R) and the return-to-supply (R2S) configuration. When introducing a new configuration of the DH grid, continuity and momentum equations together with the thermal model have to be defined and solved again, as shown in Fig. 3. Detail description and graphical presentation of the connection configurations is given in Section 3.2.

To improve the performance of the DH grid, a reference and two alternative scenarios were analyzed in this study for both connection configurations of the prosumer, R2R and R2S. In the Reference scenario, the main supply temperature was assumed to be constant through the year, while the pump control was assumed a constant frequency control. In the first alternative scenario, an improvement in the control of the supply temperature was introduced; the supply temperature was compensated by the outdoor temperature in the scenario named the outdoor temperature compensation (OTC). Finally, to improve the pressure distribution of the DH grid, the second alternative scenario with the pump control (PC) was introduced. To provide the required heat rate to each substation, a minimum pressure drop of 0.7 bar at each customer substation should be provided, meaning that the farthest substation from the main heat supply should have an available pressure difference of 0.7 bar. For the PC strategy, the pump was controlled to maintain the constant pressure difference over the pump of 3 bar. The introduced boundary conditions are given in Table 2.

Finally, the entire calculation approach in this study consisted of the following. For each connection configuration of the prosumer, R2R and R2S, the test cases with different flow rates through the prosumer (Case 1 to 3 in Table 1) together with the scenarios for the improvement (Reference, OTC, and PC) were simulated by using the approach shown in Fig. 3. Consequently, by using the input vectors of heat load for each time step, hourly simulations over the entire year were performed.

3. Case study

In this section, the analyzed DH system of NTNU university campus in Trondheim, Norway, is explained. The heat loads, characteristic parameters, and prosumer characteristics are explained. According to Köppen-Geiger climate classification, Trondheim climate subtype is Dfc (Continental subarctic climate) [30,31]. In this categorization Trondheim's weather is characterized by short and cold summer with strong seasonality. Hence, the demand for heating is expectable all year around. The study in Ref. [32] mapped the renewable photovoltaic and wind energy systems worldwide. It was found that regions with climate code Dfc such as Tromsø, Norway have the largest potential for wind energy production, however with the highest capital cost. Therefore, a large portion of electricity needs could be covered by RES, making the waste heat recovery from data centers more reasonable.

3.1. Description of the campus buildings

The NTNU campus has established its own DH ring, separate from the main DH grid of Trondheim municipality by two heat exchangers. This was done in order to enable the recycling of low-grade excess heat generated in the data center. The campus' DH system utilizes two heat exchangers, to supply heating energy to 23 consumer buildings. Currently, the prosumer building is connected to export heat to the return line (the R2R configuration) of the DH system, due to the high supply temperature that was required in the existing buildings. In our case, the data center is the heat prosumer, because the same building had at the same time heat demand and delivered the waste heat to the DH grid.

Thermal requirements for the buildings were obtained by collecting heat use for each building from the energy monitoring platform from 2010 until 2016. The analysis of the campus' energy use was performed earlier in Ref. [33], and this provides more details. In the current study, the models were calibrated and tested according to heat use in 2016. The hourly heat demand of the campus and the outdoor temperature variations in this year are given in Fig. 4.

3.2. Layout of the DH network at the campus

The layout of the network with branches and nodes is shown in Fig. 5. The nodes and the branches are numbered in black and red, respectively. Node 1 is the main heat central, where the NTNU
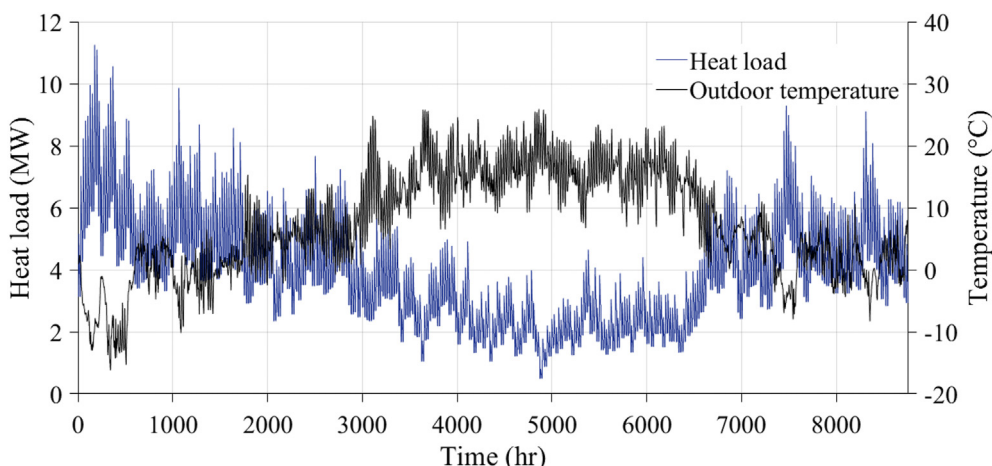
Table 2
Boundary conditions for different scenarios.

Scenario	Boundary condition
Reference	Constant frequency control
Reference	$T_1 = 75°C$
PC	$H_p = 3\ bar$
OTC	$T_1 = f(T_o)$
All scenarios	$p_1 = 1$
All scenarios	$T_{users,Ret} = T_{rp}$

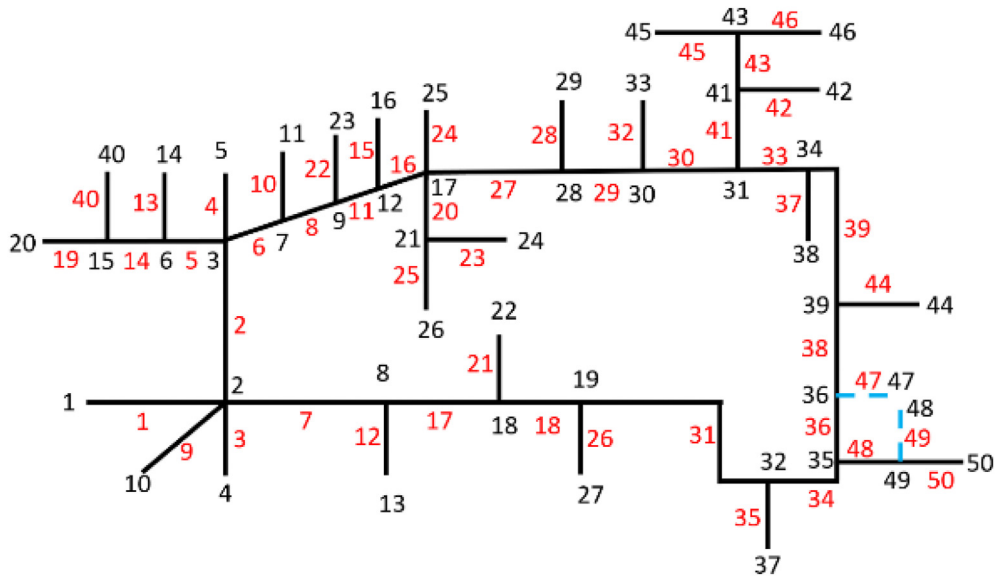**Fig. 4.** Hourly heat demand and outdoor temperature in 2016.

Fig. 5. Numeration of nodes and branches for the supply and return pipes.

campus receives the heat from the Trondheim DH system. The interaction of the data center with the campus DH grid was calculated at the two nodes, 47 and 48, and for the two branches, 47 and 49, see Fig. 5, corresponding to the inlet and the outlet of the prosumer unit. To investigate the possible solutions to integrate the waste heat from the data center, two separate setups for the interfaces of the heat pump and the primary side of the campus DH ring were considered as follows:

- *R2R - Return to return configuration* − the flow from the return pipes was guided to the condenser of the heat pump at the data center. After that flow was warmed up, it was returned to the return line again. To introduce this in the model, the two additional branches in the return line were introduced, branches 49 and 47; see Fig. 5. Since the analyzed data center is the heat prosumer, using and delivering heat at the same time, nodes 47, 48, 49, and 50 were physically located in the same building, but, due to differences in the utility of the substations in this building, they were separately considered.
- *R2S - Return to supply configuration* − the flow from the return pipe was guided to the condenser of the heat pump at the data center. After that flow was warmed up, it was returned to the supply. To introduce this in the model, the connection of the

waste heat injection to the DH grid should be removed from the topology, by removing Nodes 48 and 49 and branches 49 and 50; see Fig. 5.

The maximum mass flow rates in the pipes were defined according to the mass continuity in each node and the maximum of 1.5 m/s velocity limit, to prevent stress in the pipes. The diameters of the pipe segments were determined according to the design heat demands and assuming 25 K for the design temperature difference. The pipe selected for the simulation of the case study is a single flow pipe, insulated with polyurethane foam, with reference thermal conductivity of 0.0260 W/mK at 50 °C and surface roughness of 0.045 mm.

3.3. Thermal characteristics of the heat prosumer

At the observed campus, a building built in 1975 with the area of 18 595.8 m² has been extended over time. The building consists of offices, lecture sales, and laboratories. Consequently, the building got a data center. As the result, the building is still using heat and delivering heat and thereby performing as a heat prosumer at the campus level. The hourly heat rates of the heat use and delivery of the prosumer building are shown in Fig. 6.
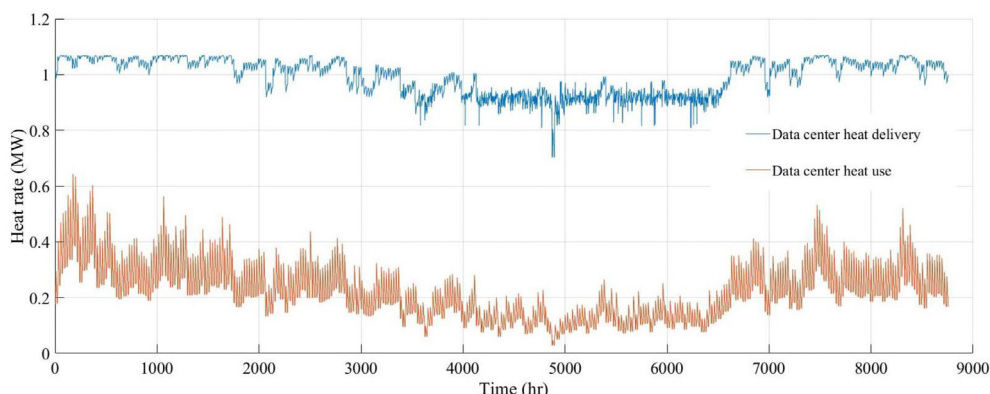

Fig. 6. Heat use and heat delivery of the prosumer building at the university campus.

From Fig. 6, it can be noted the waste heat from the data center was delivering stably to the DH ring an average heat rate of almost 1 MW, while the heat demand of the building showed seasonality. In total, the building specific annual heat use was 104 kWh/m^2, while the total annual heat delivery from the data center was 8.6 GWh per year.

Regardless of the development and initiatives to utilize the waste heat from the data centers and to consider data centers either as a third-part delivery or prosumers in DH [12], there is no yet any clear technical requirement when a building may be treated as a heat prosumer [34]. In addition, there are only a few studies such as in Ref. [17] to show directly the delivered heat rate from the prosumer as shown in Fig. 6. The review study by Huang et al. about the data centers as heat prosumers showed a detail list with many different prosumer examples, but there is no clear indication the real achieved numbers [12]. In this study, the starting points were made based on the real measurements and really achieved heat amounts.

4. Results

The results of the analyses how the heat prosumer affects the DH network performance are presented in this section. The focuses of the analyses were on the possible benefits and issues for the analyzed scenarios. These may be further used for the development of new circulation pump control strategies and improvement in the system sizing.

4.1. Thermal characteristics of the DH grid

The analysis of the thermal characteristics included the following analyses: the temperature level at each node in the DH grid, the return temperature at the main heating central, and the temperature difference at some important consumer substations. The analysis of the thermal characteristics included analysis of the different prosumer connection configurations, the different control strategies, and the different waste heat amounts; please see the section on the simulation setup and Table 1.

The results for a typical winter and summer day for the temperature at each node for the two different connection configurations are given in Fig. 7.

The results in Fig. 7 show that the introduction of the heat prosumer to the DH grid caused fluctuations in the temperature level of the DH grid. For the R2R configuration, the highest deviation from the expected average temperature was observed at Node 37, which was the closest to the data center. The temperature deviation was the smallest at Node 1, which was the farthest from the data center. The most affected nodes were located close to the data center. The return temperature at the main heat central for the R2R configuration severely increased for the low heat demand conditions (marked 'summer' in Fig. 7), as a result of the low heat delivery from the main heat central but the high heat injection in the return line from the heat prosumer. For the R2S configuration, the temperature distribution in the DH network was highly dependent on which heat source was delivering most of the heat for the university DH ring. In high heat demand and low heat demand
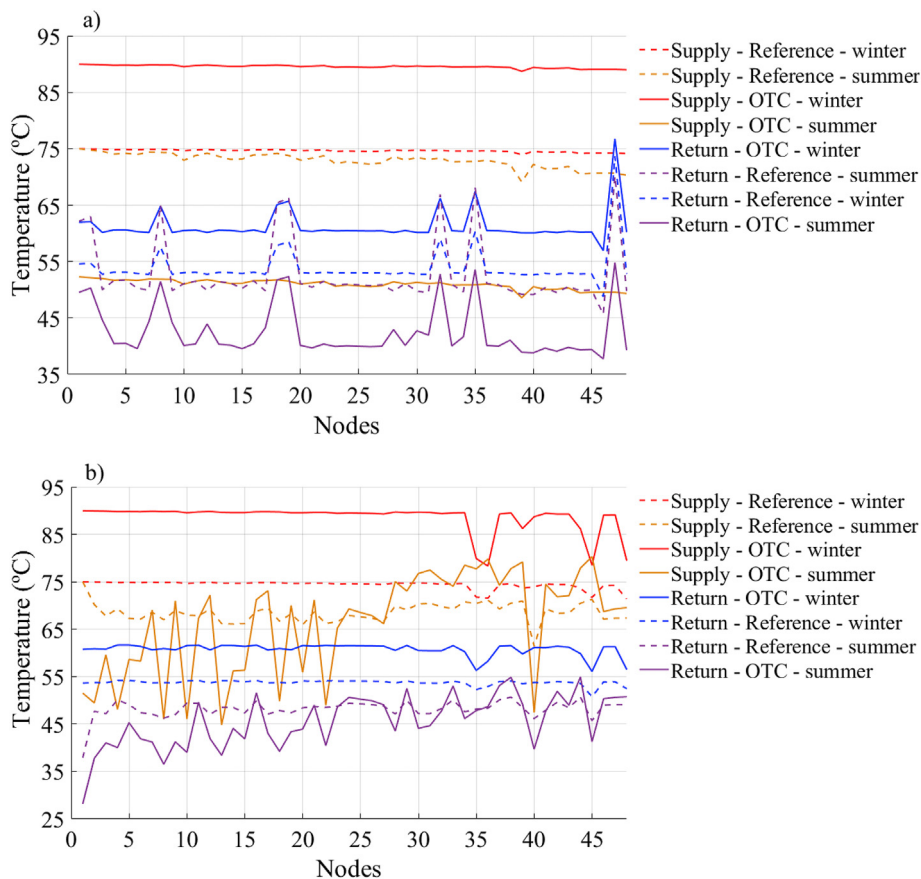

Fig. 7. Temperature distribution for analyzed scenarios: a) the R2R configuration, b) the R2S configuration.

conditions, the waste heat source covers roughly 10% and 87% of the total heat demand, respectively. The supply temperature in the Reference scenario was 75 °C. The waste heat was supplied at a temperature of nearly 70 °C in the high demand condition (marked 'winter' in Fig. 7b). Therefore, due to the high average supply temperature in the DH grid, the introduction of the waste heat had the least effects on the nearby nodes; see Fig. 7b. For the same condition and for the OTC scenario, where the supply temperature was nearly 90 °C, the waste heat temperature was almost 80 °C. This reduced the temperature of nearby nodes more than in the Reference scenario. In the OTC scenario, this temperature reduction effect was more obvious, because the waste heat source was not able to cope with the outdoor compensated supply temperature in colder conditions and, thereby, resulted in low-grade supply heat for nearby consumers. However, in the low demand condition (marked 'summer' in Fig. 7b), for the Reference scenario, even though the temperature of the supplied waste heat was still lower than the main supply temperature, the waste heat provided enough heat. Lowering the main supply temperature in the OTC scenario, together with the lower heat demand in the warm season, contributed to a successful utilization of the waste heat for most customers. However, for the R2S configuration and the OTC scenario, the nodes in the supply line were still under the effect of the waste heat injection, but the return temperatures experienced minor impacts; see Fig. 7b.

Regarding the interaction with the main DH system in Trondheim, it is very important to provide a low return temperature for many reasons, such as lowering the distribution losses, less pump power, and better utilization of heat sources. Therefore, the analysis of the return temperature was performed to identify which prosumer configuration and control may help lower the return temperature, as shown in Fig. 8. The results in Fig. 8 included the values for different heat amounts and flow rates of the waste heat; please see Table 1 in the section on the simulation setup. The results in Fig. 8 clearly show the effects of scenarios and adopting different configurations. In the R2R configuration for the Reference scenario,

the return temperature was mostly in the range of 55−60 °C, which was higher than the design condition. However, the real measurements of the return temperature showed the same trend. Increasing the share of the waste heat for Case 3 decreased the return temperature for both configuration scenarios and both control strategies. For the R2S configuration, the first considerable difference compared to the R2R configuration is the range of the return temperature at the main heat central. For the Reference scenario, the return temperature tended to be maintained in the range of 50−55 °C for most hours. However, for the rest of the hours, a decrease in the range was evident, because of the dominant influence of the waste heat source; see Fig. 8a. In addition, in the OTC scenario, the return temperature even reduced to 25−30 °C and 30−35 °C for some hours, as a result of both lowering the temperature level in the main grid and relying on the waste heat. Increasing the share of the waste heat resulted in a reduction in the return temperature.

Good water cooling or high temperature difference between the supply and the return temperature in a consumer substation is a sign of the proper operation of a substation [35,36]. The temperature differences for the two consumer substations, one close to the waste heat source (Node 37) and one far from the waste heat source (Node 40), are shown in Fig. 9. To recall, to see the nodes' positions, please see Fig. 5. In the R2R configuration, the temperature difference at the observed substations was only affected by the heat supplied by the main heat central. This meant that the increase in the share of the waste heat injection to the return line would not make significant temperature changes. Therefore, only the results for Case 1 for the R2R configuration are shown in Fig. 9. For the Reference scenario, the temperature difference was between 15 and 25 K. However, for the OTC scenario, the temperature difference achieved even 5−10 K in Node 37. Node 40 in the R2S configuration experienced relatively higher temperature differences than Node 37. The temperature differences for Node 40 might be treated as good, even though slightly higher differences would be beneficial. For the low heat demand conditions, Node 40 had a
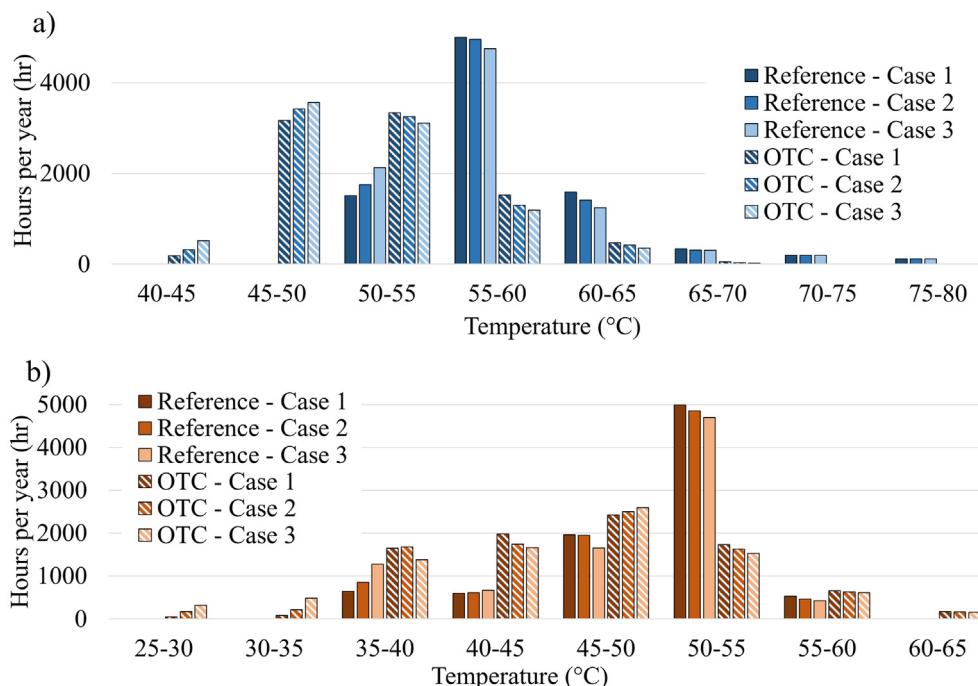

Fig. 8. Analysis of the return temperature at the main heat central for a) R2R configuration and b) R2S configuration.
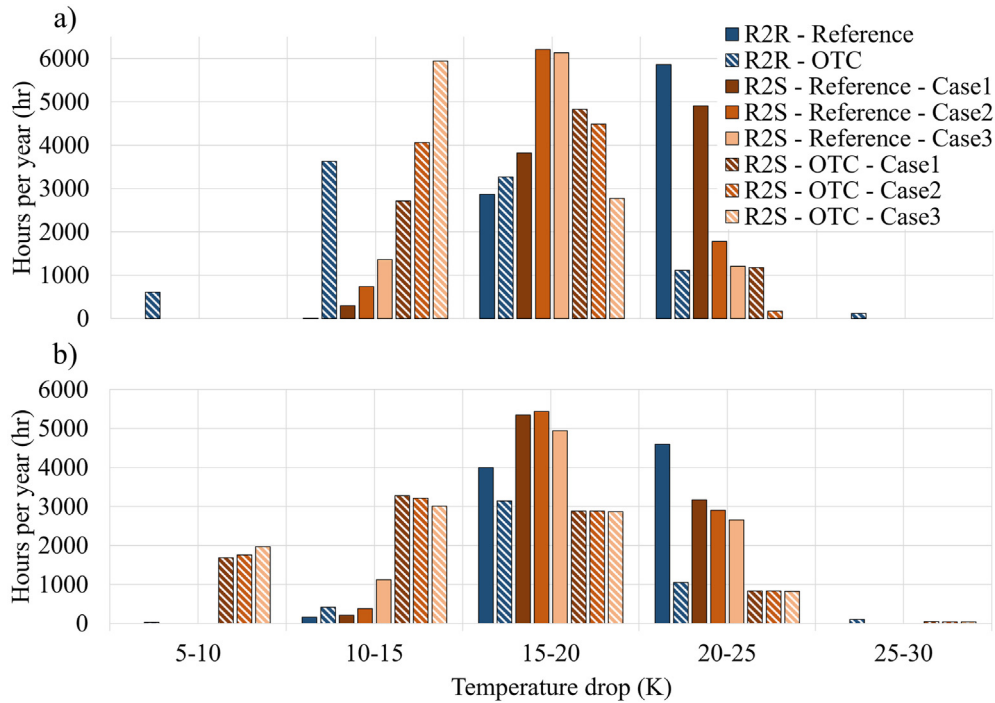
Fig. 9. Analysis of the temperature difference at consumer substations: a) Node 37 and b) Node 40.

lower temperature difference compared to Node 37. Further, due to the lower supply temperature and dependency on the waste heat, this difference was increased by adopting the OTC scenario.

4.2. Hydraulic analysis of the DH network

To enable desirable and reliable flow rates to each consumer substation in the DH grid, including the heat prosumer, it was necessary to analyze the pressure level in the DH grid. As explained in Section 2.1 and with Equations (12) and (13), it was possible to analyze the pressure level and the pressure difference in the DH grid. The flow movement toward the farthest point of the DH network creates pressure gradients, due to friction and hydraulic

losses that lead to the pressure drop. The results on the pressure level in the supply and return lines of the campus DH ring for a typical winter day are given in Fig. 10. Please note that, in Fig. 10, the pressure levels for the R2R configuration are given in the upper part, while, for the R2S, they are given in the lower part of Fig. 10, for all the control strategies introduced in Section 2.5. To calculate the pressure level and the pressure drop in Fig. 10, the models were calibrated based on the measurement data and the assumption about the pressure drop per unit of the pipe length. Before the pressure levels in the DH ring with the prosumer are presented, it is important to note that the R2S configuration changes the flow picture and how a streamline looks. In a traditional DH system with only one central heat supply plant, there is a clear difference
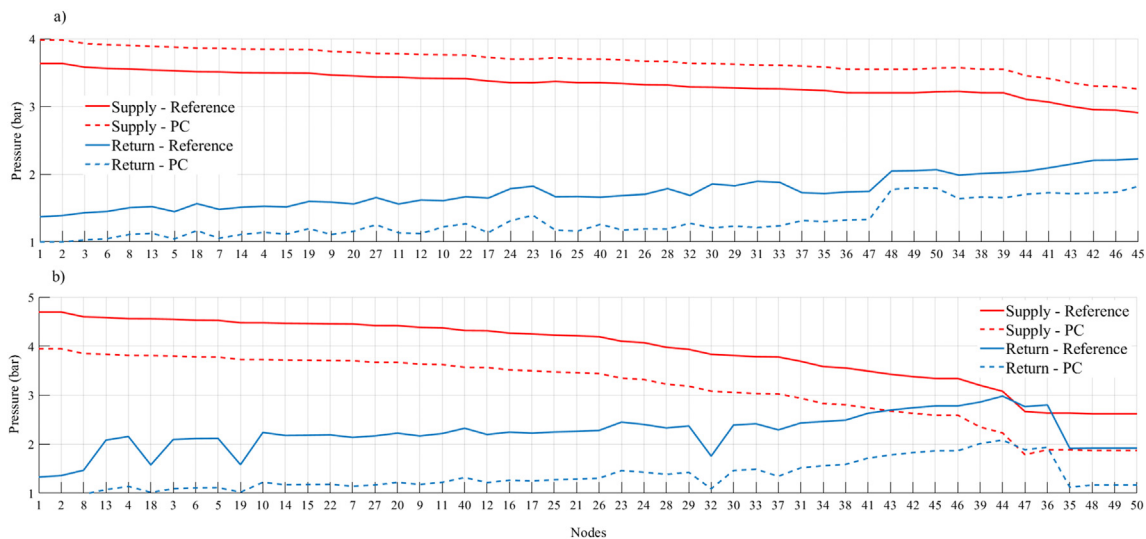

Fig. 10. Pressure level in the network for the supply and the return line a) R2R configuration, b) R2S configuration.

between the supply and the return line and, therefore, the pressure levels are presented in that way [24]. Therefore, in Fig. 10, the results are presented by following the streamline and not the ordinal number of the nodes in Fig. 5.

Fig. 10 shows that pressure changes took place close to the prosumer, specifically in Node 37, which was the consumer sub-station closest to the prosumer; see Fig. 5. The pressure level in the return line of the R2R configuration decreased after the heat prosumer, due to waste heat injection and the pressure drop through the prosumer. This meant that the pressure level in the return line would be lower than without a prosumer and it would cause higher pressure differences for all the consumers after the prosumer. This may be observed by the drop in the return line in Fig. 10a for the R2R configuration. When introducing the PC strategy, the pressure level in the return line was lower for the R2R configuration than with the Reference scenarios. The reason for this was that the PC strategy provided enough pressure difference in the system and at the farthest consumer. The Reference scenario with the constant frequency pump control did not provide enough pressure difference of 0.7 bar at the farthest consumer. This might cause the farthest consumer to sometimes not obtain the desired flow rate, in the Reference scenario. When introducing a heat prosumer with the R2S configuration, the return nodes before the prosumer will hydraulically become the nodes in the supply line. This is the reason why the pressure level close to the prosumer in the return line was higher than in the supply for the R2S configuration; see Fig. 10b. Further, in Fig. 10b, it can be noted that the effect of the waste heat injection on the pressure level at the nearby point was significant for the R2S configuration. The pressure decreases in the supply line due to the waste heat injection in the supply, R2S, led to less available pressure differences for the buildings after the waste heat injection.

After the pressure level analyses, it was possible to analyze the pressure differences at all the substations. The pressure difference analysis is important for understanding the available pressure for the flow rate control of the consumer substation. As mentioned before, the minimum of 0.7 bar pressure difference was required at the user substations. However, the pressure drop difference was sometimes below this limit during certain hours of the year, under the Reference scenario in the R2R configuration. Fig. 11 shows the analysis of this problem for Node 37 over one year.

Fig. 11 shows that the pressure difference at Node 37 was below the minimum value when the waste heat injection increased. This means that, during the months with low heating demand, the low pressure difference problem was evident. This happened due to the

lower flow rate in the network. The low flow rate made the pressure from the data center disturb the hydraulic balance of the nearby users more than under the high heat demand conditions. Under the high demand conditions, the pressure difference was followed by a general pressure drop in the system. This problem of the low pressure difference was partially avoided with the PC strategy. Finally, this problem was a bit less in the R2S configuration and the PC strategy; see Fig. 11. The results in Fig. 11 show that the R2R configuration gave higher pressure differences during certain hours. High pressure differences over the consumer substation would also decrease the flow control possibilities. The results in Fig. 11 show that the R2S configuration gave a better pressure difference range, regardless of the control method.

4.3. Energy analysis of the DH grid with the heat prosumer

The results on obtained waste heat amount, temperature levels, heat losses, and the overall annual performance are presented here for the analyzed scenarios and the prosumer configurations. Firstly, the results organized on a monthly level are presented and then the annual performance is given. Fig. 12 illustrates the amount of waste heat obtained in each month.

The results in Fig. 12 show that, for most of the cases, the obtained waste heat decreased in the warmer months, except for the two cases in the Reference scenario for the R2S configuration. The reason for this increase in the obtained waste heat for Cases 2 and 3 was the high share of the waste heat in the DH network. However, regardless of the high heat amount, the temperature level of the waste heat might be an issue. During the warmer months, the waste heat did not necessarily provide the best heat quality regarding the temperature level as shown in Fig. 13. The results in Fig. 13 show that Cases 2 and 3 in the Reference scenario for the R2S configuration provided very low waste heat temperature, 50−65 °C, in a considerable number of hours. Looking at both Figs. 12 and 13, an increase in the waste heat share resulted in increased waste heat delivery, but the waste heat had lower temperature levels.

The heat losses determine the DH competitiveness [8,24]. Therefore, the heat losses were analyzed when the prosumer was included. The results showed that the waste heat utilization led to a change in heat losses within the DH network. The heat losses as the integral and percent values are given in Fig. 14. The integral values for the thermal losses in the warmer months were less than in the colder months, but their percentage share in the monthly heat demand was higher in the warmer than in the colder months; see
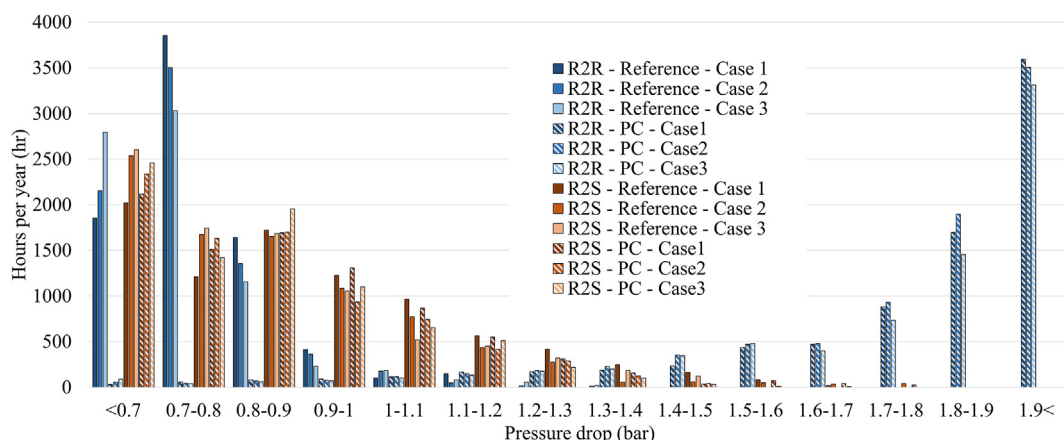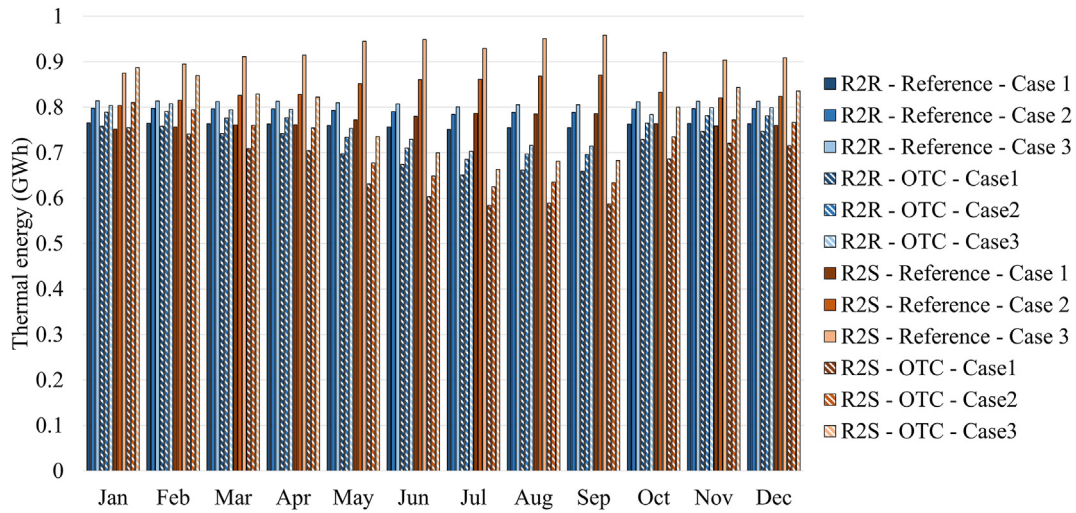

Fig. 11. Pressure difference at Node 37.

Fig. 12. Waste heat obtained from the data center per month.
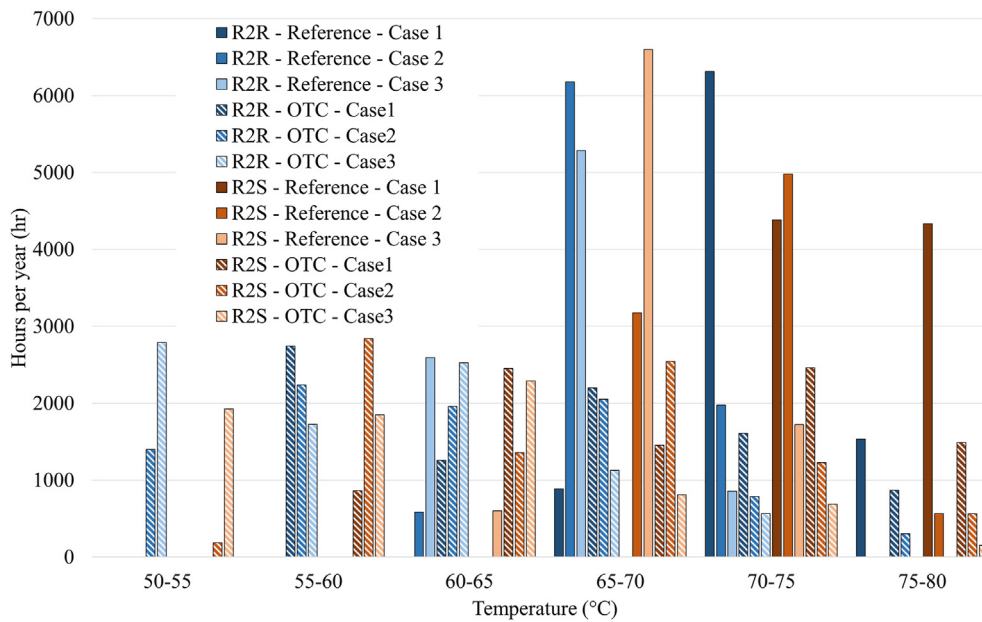

Fig. 13. Waste heat temperature range.

comparison of the upper and lower Fig. 14. Therefore, it may be concluded that the intensity of heat in the DH network had a strong impact on the DH heat losses. Increasing the share of the waste heat resulted in lower heat losses in all the analyzed scenarios, especially for the R2S configuration, where the average heat loss was generally lower than for the R2R configuration. Finally, for Case 3 in the OTC strategy and for the R2S configuration, the amount of heat loss was considerably decreased and deviated less from its average.

Finally, the overall energy performance presented as annual waste heat obtained, the total electricity, and the circulation pump use are presented below. Fig. 15 compares the obtained annual waste heat from the prosumer in the DH system under two scenarios, while Fig. 16 shows the annual amount of heating losses at the campus DH ring. The Reference scenario showed a higher amount of the obtained waste heat for both configurations. For example, the R2S configuration for the Reference scenario could harvest 19% more waste heat than the R2R configuration and

thereby saved additional 7% of the total heat use. However, as mentioned with Fig. 13, the high temperature of the waste heat was not guaranteed. The reduction in the supply temperature levels when the outdoor temperature increased led to heat recovery with the lower temperature values for the OTC strategy. As the result of this effect, the contribution of the waste heat to cover the campus heat demand gradually increased with the increase in the flow rate through the prosumer; see Case 3 in Fig. 15. The configuration change from R2R to R2S caused increase in the harvested waste heat and this effect was higher for the Reference scenario than for the OTC. In the Reference scenario for the flow rate of Case 2, the R2S configuration could harvest 14% more than R2R.

The annual heat losses were lower when the share of the waste heat was increased and lowered by the OTC strategy; see Fig. 16, where it is possible to notice that the R2S configuration showed better results for limiting the heat losses, regardless of the increased amount of the obtained waste heat. On average for Cases
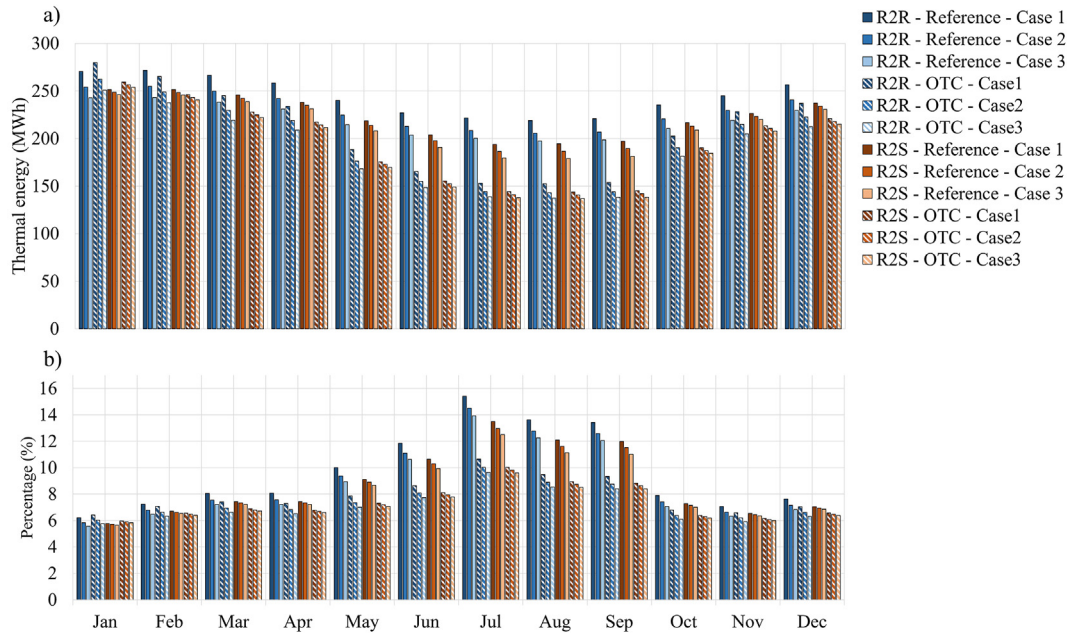
Fig. 14. Thermal energy loss in the network, a) monthly amount b) percentage of monthly demand.
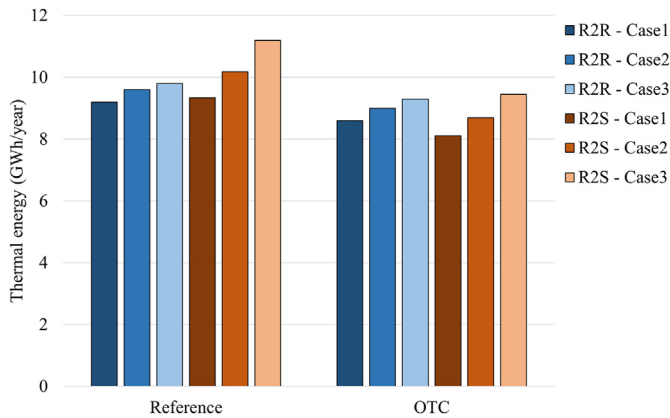

Fig. 15. Comparison of the obtained annual waste heat.
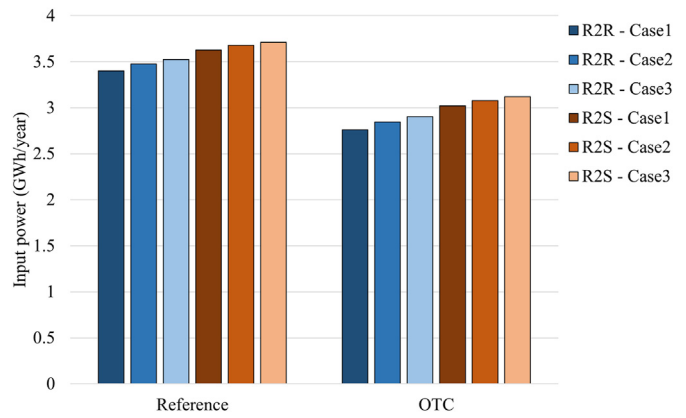

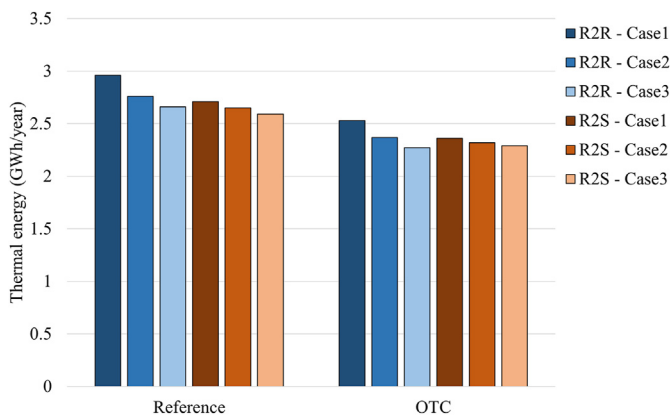**Fig. 17.** Comparison of compressor electricity use.

Fig. 16. Comparison of the annual heat losses.

1 to 3, the change from the R2R to the R2S configuration gave 4% decrease in heat losses, while the improved supply temperature control with the OTC scenario gave 14% decrease in heat losses.

The annual electricity use for the heat pump compressor and for the circulation pump in the DH network are given in Fig. 17 and Fig. 18, respectively. The amount of electricity used by the heat pump compressor depends on the return water temperature to the data center. Therefore, the compressor's electricity use was lower for the OTC scenario. Further, a very important conclusion may be drawn from Fig. 17 that, when increasing the share of the waste heat (from Cases 1 to 3) by increasing the flow rate toward the data center for approximately 50%, the compressor's electricity use increased very little, because the temperature levels were still the same, while the compressor power increased very slightly. Finally, the most important conclusion from Fig. 17 was that the R2S configuration only increased the compressor electricity use a little. However, as emphasized above, the OTC strategy helped to decrease the compressor power for all the scenarios. On average for Cases 1 to 3, the change from the R2R to the R2S configuration gave about 7% increase in the compressor electricity use, while the improved supply temperature control with the OTC scenario gave 17% decrease in the compressor electricity use. When observing
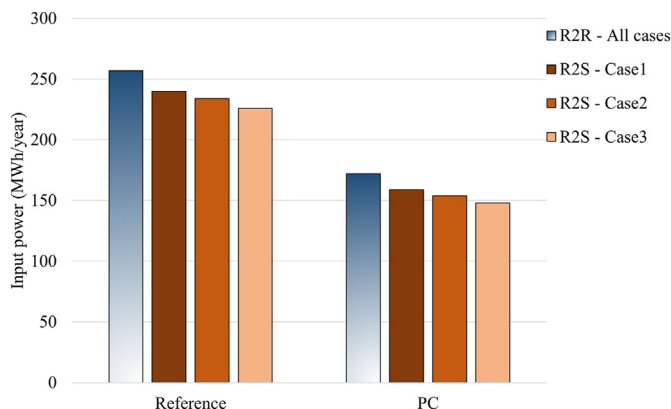
Fig. 18. Comparison of the annual electricity use for the circulation pump.

only the R2S configuration with the OTC scenario, a decrease of 15% was achieved compared to the Reference scenario.

Regarding the results in Fig. 18, it is important to point out that the annual circulation pump electricity use for the R2R configuration was not affected by the different shares of the waste heat. Therefore, the circulation pump electricity use for the R2R configuration is presented with only one column for the Reference and OTC scenarios. However, the circulation pump's electricity use for the R2S configuration showed dependency considering the waste heat amount; see Case 1 to Case 3 for the R2S in Fig. 18. Adopting the PC scenario considerably decreased the circulation pump's electricity use, because it kept the pressure difference at a constant level. Finally, the PC scenario resulted in a potential annual electricity saving for the circulation pump of 33% for the R2R configuration and 34% for the R2S configuration compared to the Reference scenario. When analyzing the hourly electricity use of the circulation pump, it was found that, despite at times slight increases in the maximum circulation pump power under the PC scenario, the pump's electricity use reduced. This could be an advantage for controlling the pressure cones of the prosumer, specifically when the heat demand of the DH network is low, and the effect of the prosumer is more significant at nearby nodes.

5. Conclusions

The study analyzed the operation of a data center as a heat prosumer for the DH ring on the university campus in Trondheim. The thermal and hydraulic behavior of the DH grid was investigated, considering real operation data for one year. The aim of the study was to develop data informed physical models for simulation of DH grids for better presentation of hydraulic and thermal aspects in the DH grids integrating heat prosumers.

The analysis identified that utilization of the waste heat from the local heat prosumer had both advantages and limitations. The analysis of the hydraulic model showed that the heat prosumer as a secondary heat source produced its own pressure cone in the DH network. Further, it was found that the heat prosumer had a negative effect on the differential pressure of the nearby customer substation. The effect scaled up when the share of the waste heat to the DH grid increased. However, the implementation of the variable frequency control for the circulation pump resulted in an improvement in the pressure balance for the nearby consumer substation. Finally, the improved pump control resulted in a potential annual electricity saving of 33% for the R2R configuration and 34% for the R2S configuration compared to the Reference scenario.

The results of the study showed that the supply temperature control reduced the heat losses and thereby increased the advantages of the DH system. Further, the lower temperature levels resulted in higher waste heat utilization. It was revealed that the higher share of circulating water in the heat prosumer caused a reduction in the water temperature introduced by the waste heat source. A very important conclusion for this study is related to the DH return temperature. The analysis of the return temperature showed that the R2S configuration resulted in a lower return temperature. Finally, increasing the share of the waste heat decreased the return temperature for both configurations, R2R and R2S, and both control strategies.

The comparison of the R2R and R2S configurations to integrate the heat prosumer showed that the increase in the electricity use of the heat pump's compressor was not significant for the R2S configuration. For example, the average increase of the compressor electricity use was 7%, while implementation of the OTC scenario gave a decrease of the compressor electricity use of 17%. This is important, because the R2S configuration showed better performance regarding achieving the lower return temperature to the DH system and better pressure difference over the nearby consumer substation.

Finally, integration of the heat prosumer could be advantageous on the way to a renewable society, if relevant measures regarding the pressure and the temperature control were considered. As shown in the achieved waste heat, the configuration change from R2R to R2S caused gave up to 7% lower total heat supply.

The results of the study may be used to identify the potentials and how to integrate a heat prosumer in the existing DH system. Further, the results may be used to find new and innovative solutions for the pressure and temperature control. Future work will consider an integrated pressure and flow control between the circulation pump and control valves in the buildings.

Although a few assumptions were introduced for the models, all the introduced models were calibrated with the measured data, and the achieved operation results were presented in detail. Therefore, the main conclusions and the trends from this study may be treated as valid and relevant for considering the integration of heat prosumers to DH systems.

Credit author statement

Natasa Nord — Organized the data measurement and collection. Prepare all the previous and background data for the study. Develop the study concept and the idea. Suggested the model development. Quality control of the results. Write and read the paper. **Mohammad Shakerin** — Analyzed the measured data. Develop hydraulic and thermal model in MATLAB. Wrote the manuscript. **Tymofii Tereshchenko** - Quality control of the results. Organized the results. Write and read the paper. **Vittorio Verda** — Help in the model developing. Quality control of the results. Read the manuscript. **Romano Borchiellini** - Help in the model developing. Quality control of the results.

Declaration of competing interest

The authors declare that they have no known competing financial interests or personal relationships that could have appeared to influence the work reported in this paper.

Acknowledgement

References

[1] Union E, editor. On the promotion of the use of energy from renewable sources, directive 2009/32/28 of the European parliament and of the Council. Brussels: Official Journal of the European Communities; 2010.

[2] Lund H, Möller B, Mathiesen BV, Dyrelund A. The role of district heating in future renewable energy systems. Energy 2010;35(3):1381—90.

[3] Buffa S, Cozzini M, D'Antoni M, Baratieri M, Fedrizzi R. 5th generation district heating and cooling systems: a review of existing cases in Europe. Renew Sustain Energy Rev 2019;104:504—22.

[4] Directive ERE. Proposal for a Directive of the European Parliament and of the Council on the promotion and use of energy from renewable sources. COM; 2008. p. 19. 2008.

[5] Guelpa E, Verda V. Thermal energy storage in district heating and cooling systems: a review. Applied Energy; 2019. p. 252.

[6] Guelpa E, Marincioni L. Demand side management in district heating systems by innovative control. Energy 2019;188.

[7] Werner S. International review of district heating and cooling. Energy 2017;137:617—31.

[8] Frederiksen S, Werner S. District heating and cooling. Lund: Studentlitteratur; 2013.

[9] Lake A, Rezaie B, Beyerlein S. Review of district heating and cooling systems for a sustainable future. Renew Sustain Energy Rev 2017;67(Supplement C): 417—25.

[10] Nord N, Schmidt D, Kallert A, Svendsen S. Improved interfaces for enabling integration of low temperature and distributed heat sources — requirements and examples. In: CLIMA 2016. Denmark: Aalborg; 2016.

[11] H Lund SW, Wiltshire R, Svendsen S, Thorsen JE, Hvelplund F, Mathiesen BV. 4th generation district heating (4GDH). Energy; 2014.

[12] Huang P, Copertaro B, Zhang X, Shen J, Löfgren I, Rönnelid M, Fahlen J, Andersson D, Svanfeldt M. A review of data centers as prosumers in district energy systems: renewable energy integration and waste heat reuse for district heating. Appl Energy 2020;258:114109.

[13] Sentralbyrå NS. Statistical yearbook of Norway/District heating: statistisk sentralbyrå.

[14] Brange L, Englund J, Lauenburg P. Prosumers in district heating networks — a Swedish case study. Appl Energy 2016;164(Supplement C):492—500.

[15] Brand L, Calvén A, Englund J, Landersjö H, Lauenburg P. Smart district heating networks — a simulation study of prosumers' impact on technical parameters in distribution networks. Appl Energy 2014;129:39—48. 0.

[16] Di Pietra B, Zanghirella F, Puglisi G. An evaluation of distributed solar thermal "net metering" in small-scale district heating systems. Energy Procedia 2015;78(Supplement C):1859—64.

[17] Kauko H, Kvalsvik KH, Rohde D, Nord N, Utne Å. Dynamic modeling of local district heating grids with prosumers: a case study for Norway. Energy 2018;151:261—71.

[18] Wang D, Orehounig K, Carmeliet J. A study of district heating systems with solar thermal based prosumers. Energy Procedia; 2018. p. 132—40.

[19] Guelpa E, Verda V. Model for optimal malfunction management in extended district heating networks. Appl Energy 2018;230:519—30.

[20] Sciacovelli A, Borchiellini R, Verda V. Numerical design of thermal systems. CLUT; 2013.

[21] Stevanovic VD, Prica S, Maslovaric B, Zivkovic B, Nikodijevic S. Efficient numerical method for district heating system hydraulics. Energy Convers Manag 2007;48(5):1536—43.

[22] Grosswindhager S, Voigt A, Kozek M. Efficient physical modelling of district heating networks. Modelling and Simulation; 2011.

[23] Haiyan L, Valdimarsson P. District heating modelling and simulation. Thirty-fourth workshop on geothermal reservoir engineering. 2009.

[24] Nord N, Løve Nielsen EK, Kauko H, Tereshchenko T. Challenges and potentials for low-temperature district heating implementation in Norway. Energy 2018;151:889—902.

[25] Vitec, NetSim grid simulation, in.

[26] West DB. Introduction to graph theory. Saddle River: Prentice hall Upper; 2001.

[27] Bondy JA, Murty USR. Graph theory with applications. Macmillan London; 1976.

[28] Patankar S. Numerical heat transfer and fluid flow. CRC press; 1980.

[29] Quarteroni A, Saleri F, Sacco R. Numerical mathematics. 2007.

[30] Chen D, Chen HW. Using the Köppen classification to quantify climate variation and change: an example for 1901-2010. Environmental Development 2013;6(1):69—79.

[31] Encyclopædia britannica, encyclopædia britannica, in.

[32] Mazzeo D, Matera N, De Luca P, Baglivo C, Maria Congedo P, Oliveti G. Worldwide geographical mapping and optimization of stand-alone and grid-connected hybrid renewable system techno-economic performance across Köppen-Geiger climates. Appl Energy 2020:276.

[33] Guan J, Nord N, Chen S. Energy planning of university campus building complex: energy usage and coincidental analysis of individual buildings with a case study. Energy Build 2016;124:99—111.

[34] Schmidt D, Kallert A, Blesl M, Svendsen S, Li H, Nord N, Sipilä K. Low temperature district heating for future energy systems. Energy Procedia 2017;116(Supplement C):26—38.

[35] Gadd H, Werner S. Fault detection in district heating substations. Appl Energy 2015;157:51—9.

[36] Gadd H, Werner S. Achieving low return temperatures from district heating substations. Appl Energy 2014;136:59—67.